RSC Advances

PAPER

View Article Online
View Journal | View Issue

Cite this: *RSC Adv.*, 2020, **10**, 6088

Thermally induced fragmentation of nanoscale calcite†

Mihiro Takasaki, Makoto Tago, Yuya Oaki and Hiroaki Imai *

Received 16th December 2019
Accepted 2nd February 2020

DOI: 10.1039/c9ra10564f

rsc.li/rsc-advances

Calcite nanorods ~50 nm wide are thermally separated into nanoblocks. The fragmentation is ascribed to the ion diffusion on metastable crystal surfaces at temperatures (~400 °C) much lower than the melting point. The presence of water molecules enhances the surface diffusion and induces deformation of the nanorods even at ~60 °C.

Calcium carbonate is a common industrial material that is used as a micrometric filler for papers, rubbers, plastics, and inks. The shape and size of micrometric grains are important parameters that affect the physical and chemical properties of composite materials.[1–5] In recent years, nanometric particles of calcium carbonate have attracted much attention as basal building blocks of biogenic minerals[6–10] and functional materials with high biocompatibility and low environmental load.[11–14] Since various properties are influenced by the miniaturization of crystal grains below 100 nm, characterization of the carbonate particles is necessary for application in practical fields. However, their properties, including the thermal characteristics of nanometric calcium carbonate in the nanometric region, have not been sufficiently clarified because calcium carbonate is easily decomposed above 550 °C.[15,16] In the present work, we studied thermally induced deformation on nanometric calcite at temperatures lower than the melting point (1597 °C at 3 GPa)[17] of the bulky crystal.

Since the melting temperature of metals decreases when their size is decreased below ~50 nm,[18,19] metallic nanowires fragment into nanospheres at temperatures much below the melting point of bulk metal.[20–22] The fragmentation is ascribed to the Rayleigh instability that is known for liquid. These results suggest that the surface diffusion of ions and atoms occurs easily on the nanometric particles when the surface instability is increased. The cleavage of solid nanowires has been observed only for metallic phases. In the current work, we found the morphological transformation of ion crystal nanorods into faceted nanograins through the surface diffusion at relatively low temperatures.

The preparation of bulky calcium carbonate consisting of nanocrystals is required for reinforcing materials[23–25] and as a precursor of biomedical materials.[26,27] In general, however, fabricating large, bulky bodies through conventional sintering techniques is difficult because calcium carbonate is thermally decomposed into calcium oxide and carbon dioxide. Several methods, such as sintering with a flux[16,28] or in a carbon dioxide atmosphere[29] and hot-pressing under hydrothermal conditions[30,31] were developed to prepare bulky calcium carbonate materials. On the other hand, the thermal behaviors of pure calcium carbonate have not been sufficiently studied at temperatures below the decomposition and melting points.

In nature, bulky calcium carbonate crystals are commonly produced as biominerals, such as shells, eggshells, sea urchins, and foraminiferal skeletons, under mild conditions.[3,9,10,32–34] The bulky biogenic bodies are composed of nanometric grains 10–100 nm in size that are arranged in the same crystallographic direction.[3] The formation of bridged architectures through oriented attachment is generally related to the ion diffusion on specific surfaces at relatively low temperatures. A detailed study on the stability of nanometric surfaces at relatively low temperatures is needed to understand the morphological change of calcium carbonate crystals.

In the present report, we discuss the morphological change of calcite nanocrystals below the decomposition and melting temperatures by observing metastable crystal surfaces in the nanometer-scale range. Calcite nanorods elongated in the *c* direction were utilized as a typical nanometric shape covered with metastable surfaces. Here, thermally induced fragmentation was studied with and without water vapor. The surface diffusion was found to occur on the metastable surface at around 400 °C under a dry condition and at around 60 °C with water vapor. Our findings are important for clarification of the surface property of nanometric calcium carbonate and for the fabrication of bulky bodies through the attachment of nanocrystals.

Single-crystal calcite nanorods elongated in the *c* direction were utilized in the present study (Fig. 1 and S1†). Calcite nanorods up to ~500 nm were formed through the combination of the carbonation of calcium hydroxide and the subsequent oriented attachment of resultant calcite nanoblocks ~50 nm in diameter by stirring. The detailed mechanism was described in

Department of Applied Chemistry, Faculty of Science and Technology, Keio University, 3-14-1 Hiyoshi, Kohoku-ku, Yokohama 223-8522, Japan. E-mail: hiroaki@applc.keio.ac.jp

† Electronic supplementary information (ESI) available: Experimental procedures. See DOI: 10.1039/c9ra10564f

our previous study.[35] As shown in Fig. S1,† the calcite nanorods were covered with metastable surfaces having a curvature. Moreover, we observed depressed parts originating from the oriented attachment of the original calcite grains. As shown in the Fig. S2,† the XRD peaks of the nanorods were found to shift to higher angles than those of standard X-ray diffraction data (ICDD 00-005-0586). Thus, the crystal lattice of the nanorods was suggested to be stressed with the coverage of irregular surfaces.

As shown in Fig. 2, the calcite nanorods were deposited on a silicon substrate for clear observation of the morphological change. We redispersed the calcite nanorods in ethanol and evaporated the dispersion medium to deposit them on the substrate at 25 °C (Fig. 2a and S3a†).[36] The nanorods were arranged on the solid surface through evaporation-driven self-assembly. Specifically, monolayers of the calcite nanorods were obtained by adding poly(acrylic acid) (PAA, MW: 5000 $gmol^{-1}$) to the ethanol dispersion. The dispersibility of the nanorods in ethanol was improved by the modifying agent. The organic components of the PAA-modified nanorods were removed through oxidation in air at around 300 °C (Fig. S4†).

The calcite nanorods were deposited on the solid surface to study the morphological change when heated in air. Obvious changes were not found in the shape of the nanorods upon heating to a temperature below 350 °C in air for 24 h (Fig. S2†). On the other hand, we observed significant deformation upon heating to 400 °C (Fig. 2). The depressed parts on the side surfaces enlarged in 1 h. The fragmentation of the nanorods was finally induced after treatment for 2 h. Calcite grains were formed by the thermally induced cleavage (Fig. 2c). The average size of the cleaved grains was ~100 nm, which was larger than the average width of the nanorods, ~50 nm. As shown in Fig. 3, we observed the definite surfaces covering nanograins. Most of the definite facets were assigned to the (104) of calcite by FFT analysis of the lattice fringes of nanograins in the HRTEM images. Some (012) planes were found in the nanograins. On the other hand, the surfaces of the deformed nanorods during fragmentation were curved and irregular. According to XRD patterns, the crystal phase was not changed with the fragmentation (Fig. S2†). The diffraction peaks were shifted to the standard values and sharpened with the treatments. This suggests that the formation of the stable faces with the fragmentation is associated with the lattice relaxation.

We observed the stability of rhombohedral grains that were covered with the stable {104} planes. As shown in Fig. 4, the deformation of the rhombohedral grains was not observed at

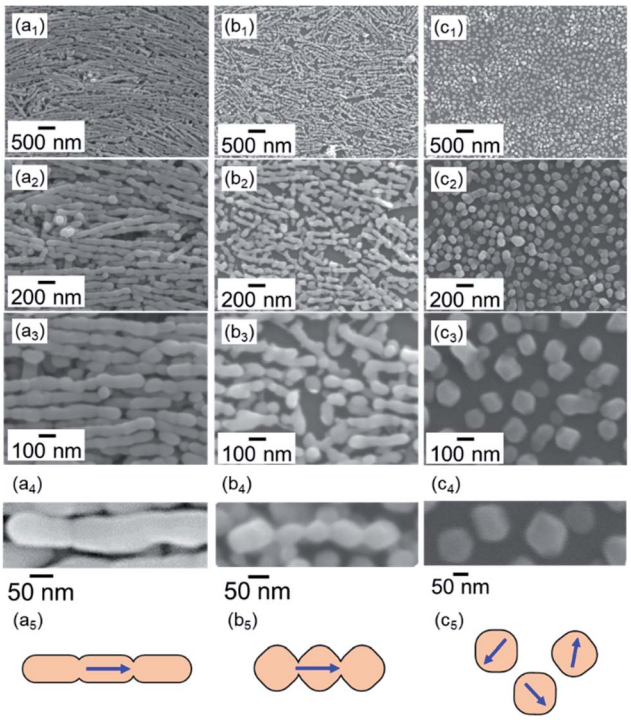

Fig. 2 SEM images and schematic illustrations of calcite nanorods deposited on a silicon substrate before treatment (a) and heated at 400 °C for 1 (b) and 2 h (c). The PAA-modified calcite nanorods were used to obtain the monolayers (b and c). We used bare nanorods for take the images of original nanorods because the definite surfaces were not observed due to the presence of PAA (a).

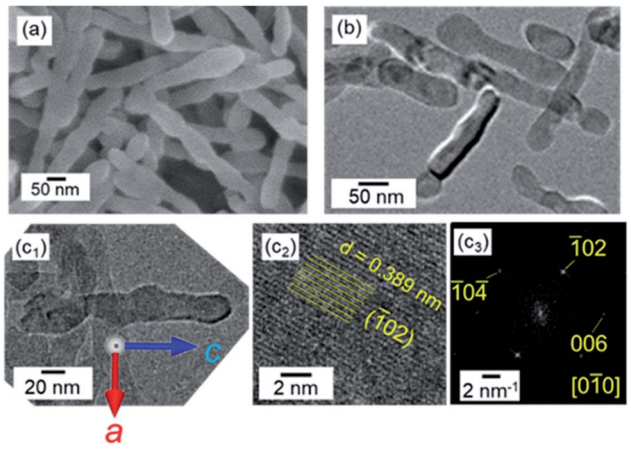

Fig. 1 SEM (a) and TEM (b and c_1), HRTEM (c_2) images, and the FFT pattern (c_3) of the lattice in (c_2) of calcite nanorods in aqueous dispersions at pH 12 and at 25 °C with stirring. (c) Reprinted from ref. 35 published by The Royal Society of Chemistry.

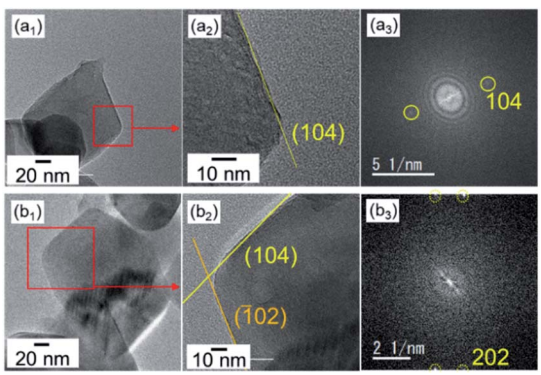

Fig. 3 TEM (a), HRTEM (b), and FFT images of nanocrystals before and after heating at 500 °C.

400 °C in air for 6 h. These results indicate that the ion diffusion is not induced drastically on the stable surfaces at a temperature lower than the decomposition temperature.

The fragmentation of the calcite nanorods was enhanced in the presence of water vapor. As shown in Fig. 5a, we found cleavage of the nanorods even at 60 °C in a closed vessel containing water. The formation of unifaceted rhombohedral nanoblocks with {104} faces was clearly observed at 100 °C for 24 h (Fig. 5b–d). Since the morphological change was similar to that under a dry condition, the ion diffusion on the surface is deduced to be assisted by adsorbed water molecules. The X-ray diffraction signals shifted to the standard values with the fragmentation (Fig. S2†). Thus, the stable faces were formed with the lattice relaxation with the exposure to water vapor.

The ion diffusion at a relatively low temperature, below the decomposition temperature, has not been reported for calcium carbonate. In the present work, however, we found the fragmentation of calcite nanorods at around 400 °C under a dry condition and at around 60 °C with water molecules. These results suggest that the ion diffusion occurs on the nanoscale calcite crystals. On the other hand, rhombohedral calcite grains covered with the stable {104} planes were not deformed at those temperatures. Thus, the diffusion at low temperatures is induced only on metastable surfaces that are exhibited on the nanoscale calcite. Moreover, the presence of water molecules enhances the ion diffusion on the metastable surfaces.

The fragmentation of the calcite nanorods can be explained by Rayleigh instability. The cleavage by Rayleigh instability is ascribed to the enlargement of tiny perturbations on cylindrical liquids,[37] polymers, and metals. In general, the cylindrical bodies evolve into several spheres to decrease the total surface energy. Recently, Rayleigh instability was applied to the thermally induced fragmentation of metal[20–22] and organic[38] nanowires. The breakup phenomena were attributed to surface oscillations due to the high surface energy induced by increased surface-to-volume ratios.[39] Thus, metal nanowires are cleaved and form isotropic nanoblocks at temperatures well below the melting point. In the present work, we found fragmentation of the calcite nanorods at relatively low temperatures. The ion diffusion is induced on the metastable surfaces that are exhibited on nanoscale crystals. The depressed parts exist as perturbations on the side faces of the original nanorods. The cleavage occurs through enlargement of the depressed parts and formation of the stable faces to reduce the surface energy and relax the lattice strain.

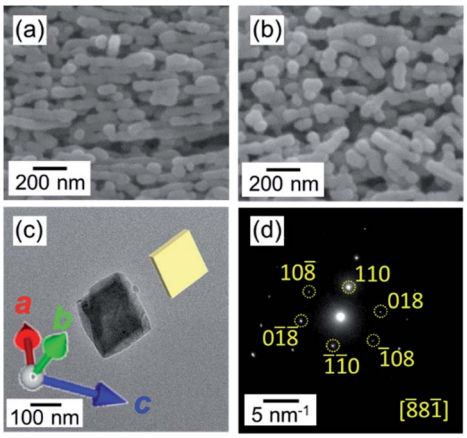

Fig. 5 SEM (a and b), TEM (c), and SAED (d) images of calcite nanorods deposited on a silicon substrate subjected to high humidity at 60 °C (a) and 100 °C (b) for 24 h. (c) A schematic illustration of a calcite rhombohedron covered with {104} faces.

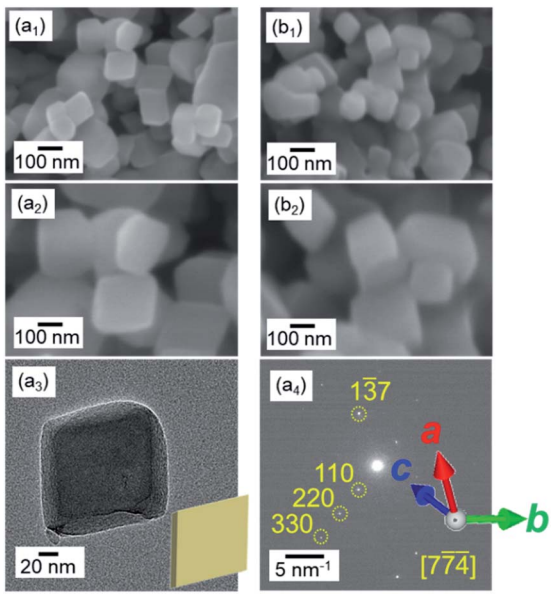

Fig. 4 SEM ($a_{1,2}$ and $b_{1,2}$), TEM (a_3), and SAED (a_4) images of calcite nanoblocks before treatment (a) and heated to 400 °C for 6 h (b). (a_3) A schematic illustration of a calcite rhombohedron covered with {104} faces.

Polyhedral grains covered with flat planes were formed instead of spherical particles by the fragmentation of calcite nanorods. Formation of the stable {104} plane is achieved to reduce the surface energy. The {012} plane of calcite is not stable under the ambient temperature. However, the surface energy of {012} decreases with increasing temperature.[40] Thus, the facets are deduced to also be formed at temperatures around 400 °C.

Conclusions

The ion diffusion of calcium carbonate was found to occur on metastable surfaces at temperatures much lower than the melting point. The fragmentation of calcite nanorods covered with metastable surfaces is ascribed to the Rayleigh instability induced by the surface ion diffusion. The presence of water molecules enhances the surface ion diffusion at temperatures lower than 100 °C.

Conflicts of interest

There are no conflicts to declare.

Acknowledgements

This work was partially supported by Grant-in-Aid for JSPS Research Fellow (JPYYK8F16), and Grant-in-Aid for Scientific Research (A) (JP16H02398) from Japan Society for the Promotion of Science.

Notes and references

1 A. L. N. Da Silva, M. C. G. Rocha, M. A. R. Moraes, C. A. R. Valente and F. M. B. Coutinho, *Polym. Test.*, 2002, **21**, 57.
2 Y. S. Thio, A. S. Argon, R. E. Cohen and M. Weinberg, *Polymer*, 2002, **43**, 3661.
3 T. D. Lam, T. V. Hoang, D. T. Quang and J. S. Kim, *Mater. Sci. Eng., A*, 2009, **501**, 87.
4 M. Bruchez, M. Moronne, P. Gin, S. Weiss and A. P. Alivisatos, *Science*, 1998, **281**, 2013.
5 Y. Liang, Y. Li, H. Wang, J. Zhou, J. Wang, T. Regier and H. Dai, *Nat. Mater.*, 2011, **10**, 780.
6 Y. Oaki, A. Kotachi, T. Miura and H. Imai, *Adv. Funct. Mater.*, 2006, **16**, 1633.
7 M. Kijima, Y. Oaki and H. Imai, *Chem.–Eur. J.*, 2011, **17**, 2828.
8 A. Hayashi, T. Watanabe and T. Nakamura, *Zoology*, 2010, **113**, 125.
9 M. Suzuki, T. Kogure, S. Weiner and L. Addadi, *Cryst. Growth Des.*, 2011, **11**, 4850.
10 S. Mann, *J. Chem. Soc., Dalton Trans.*, 1993, 1.
11 K. Fujihara, M. Kotaki and S. Ramakrishnna, *Biomaterials*, 2005, **26**, 4139.
12 F. Ishikawa, M. Murano, M. Hiraishi, T. Yamaguch, I. Tamai and A. Tsuji, *Pharm. Res.*, 2002, **19**, 1097.
13 L. F. Peng, X. X. Liu and G. Y. Yang, *China Surfactant Deterg. Cosmet.*, 2001, **5**, 13.
14 A. I. Petrov, D. V. Volodkin and G. B. Sukhorukov, *Biotechnol. Prog.*, 2005, **21**, 918.
15 F. Tetard, D. Bernache-Assollant and E. Champion, *J. Therm. Anal. Calorim.*, 1999, **56**, 1461.
16 J. Ito, Y. Matsushima, H. Unuma, N. Hiriuchi, K. Yamashita and M. Tajika, *Mater. Chem. Phys.*, 2017, **192**, 304.
17 Z. Li, J. Li, R. Lange, L. Jiachao and B. Militzer, *Earth Planet. Sci. Lett.*, 2017, **457**, 395.
18 M. Takagi, *J. Phys. Soc. Jpn.*, 1954, **9**, 359.
19 C. R. M. Wronski, *Br. J. Appl. Phys.*, 1967, **18**, 1731.
20 M. Rauber, F. Muench, M. E. Toimil-Molares and W. Ensinger, *Nanotechnology*, 2012, **23**, 475710.
21 H. Oh, J. Lee and M. Lee, *Appl. Surf. Sci.*, 2018, **427**, 65.
22 S. Karim, M. E. Toimil-Molares, A. G. Balogh, W. Ensinger, T. W. Cornelius, E. U. Khan and R. Neumann, *Nanotechnology*, 2006, **17**, 5954.
23 C. M. Chan, J. S. Wu, J. X. Li and Y. K. Cheung, *Polymer*, 2002, **43**, 2981.
24 S. C. Tjong, *Mater. Sci. Eng., R*, 2006, **53**, 73.
25 S. Y. Fu, X. Q. Feng, B. Lauke and Y. W. Mai, *Composites, Part B*, 2008, **39**, 933.
26 A. C. Tas, *Int. J. Appl. Ceram. Technol.*, 2007, **4**, 154.
27 F. Heilmann, O. C. Standard, F. A. Müller and M. Hoffman, *J. Mater. Sci.: Mater. Med.*, 2007, **18**, 1817.
28 F. Tetard, D. Bernache-Assollane, E. Champio and P. Lortholary, *Solid State Ionics*, 1997, **101**, 517.
29 F. Mouchau, T. Loanovici, P. Hivart, L. Bereteu, H. F. Hildebrand, *Eur. Conf. Biomater., 24th*, 2011, pp. 91–95.
30 N. Yamasaki, T. Weiping, K. Jiajun and K. Hosoi, *J. Mater. Sci. Lett.*, 1995, **14**, 1268.
31 D. L. Olgaard and B. Evans, *Contrib. Mineral. Petrol.*, 1988, **100**, 246.
32 M. Rousseau, E. Lopez, P. Stempfle, M. Brendle, L. Franke, A. Guette, R. Naslain and X. Bourrat, *Biomaterials*, 2005, **26**, 6254.
33 G. Friedbacher, P. K. Hansma, E. Ramli and G. D. Stucky, *Science*, 1991, **253**, 1261.
34 H. A. Lowenstam, *Science*, 1981, **211**, 1126.
35 M. Takasaki, Y. Kimura, T. Yamazaki, Y. Oaki and H. Imai, *RSC Adv.*, 2016, **6**, 61346.
36 M. Takasaki, T. S. Suzuki, Y. Oaki and H. Imai, *Nanoscale*, 2018, **10**, 22161.
37 R. Mead-Hunter, A. J. C. King and B. J. Mullins, *Langmuir*, 2012, **28**, 6731.
38 S. Mei, X. Feng and Z. Jin, *Macromolecules*, 2011, **44**, 1615.
39 S. Karim, M. E. Toimil-Molares, W. Ensinger, A. G. Balogh, T. W. Cornelius, E. U. Khan and R. Neumann, *J. Phys. D: Appl. Phys.*, 2007, **40**, 3767.
40 B. Marco, *CrystEngComm*, 2015, **17**, 2204.